Dalton Transactions

Accepted Manuscript

ROYAL SOCIETY OF CHEMISTRY

www.rsc.org/dalton

The role of the $[CpM(CO)_2]^-$ Chromophore in the Optical properties of the $[Cp_2ThMCp(CO)_2]^+$ complexes, where M=Fe, Ru and Os. Theoretical View

Plinio Cantero-López[a], Laura Le Bras[b], Dayán Páez-Hernández[a], Ramiro Arratia-Pérez[a]

[a] Relativistic Molecular Physics (ReMoPh) Group, Ph.D. Program in Molecular Physical Chemistry, Universidad Andrés Bello, Av. República 275, Santiago 8370146, Chile.

[b] Institut des Sciences Chimiques de Rennes UMR CNRS 6226, Université de Rennes 1, 35042 Rennes, France

Núcleo Milenio de Ingeniería Molecular para Catálisis y Biosensores, ICM, Chile.

Graphical Abstract

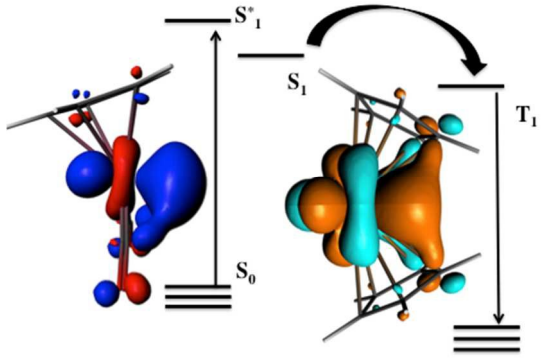

The molecules under study in the present work have an unsupported interaction between Th and transition metals (Fe, Ru, Os). This interaction is mainly ionic with some covalent character. The spin-orbit-ZORA calculation shows the possible emission of the Th complexes and the antenna effect model was employed to justify the sensitization of the actinide element by a transition metal complex.

Abstract. Chemical bond between actinide and transition metal unsupported by bridging ligands is not well characterized. In this paper we study to the electronic properties, bonding nature and optical spectra in a family of $[Cp_2ThMCp(CO)_2]^+$ complexes where M = Fe, Ru, Os, based on the relativistic two components density functional theory calculations. The Morokuma-Ziegler energy decomposition analysis shows an important ionic contribution in the Th-M interaction with around 25% of covalent character. Clearly, charge transfer occurs on Th-M bond formation, however the orbital term most likely represent a strong charge rearrangement in the fragments due to the interaction. Finally the spin-orbit-ZORA calculation shows the possible NIR emission induced by the $[FeCp(CO)_2]^-$ chromophore accomplishing the antenna effect that justify the sensitization of the actinide complexes.

1. Introduction

Metal-metal bonding is a ubiquitous feature of considerable current interest in transition-metal (M) chemistry and heterobimetallic systems, however the chemical bond between actinide and transition metal unsupported by bridging ligands is not well characterized. For homobimetallic bonds the metal-metal interaction is necessarily covalent.[1] For heterobimetallic complexes, ionic contributions to the metal-metal bond may be anticipated due to the differences in the electronegativities of the metal centers. However, the degree to which covalent contribution may be involved cannot be predicted and therefore the study of heterobimetallic compounds that do not exhibit bridging ligands, that is unsupported metal-metal bonds, is particularly attractive. [1,2] Following the first examples of unsupported An-M bonds, which include Cp_3U-$SnPh_3$ and a series of U and Th complexes with Fe and Ru reported in the 1980s, the subject fell into a period of inactivity.[2-4] Recently, this topic has returned to take an interest and some new molecules with An-M bond have been reported in the last years, being particularly relevant the work of M. Mazzanti and coworkers and S. Liddle and coworkers.[1,5-8] Formation of new metal-metal bonds with *f*-elements has been mainly achieved through metathesis or by exploiting coordinative unsaturation in starting materials. The discovery of metal-metal bonds has been of fundamental importance to the understanding of the chemical bonding and this kind of molecules could contribute to a greater understanding of the interaction between actinide elements and transition metals.[9-14].

Another important topic related to these systems is the design of compounds where the transition metal fragments bound to actinides elements act as sensitizers, resulting in the near-infrared (NIR) luminescence.[15-17]Since actinide ions are poor at absorbing light directly, due to the low extinction coefficients of the Laporte forbidden *f*→*f* transitions, energy or charge transfer from adjacent strongly absorbing transition metal chromophores has been recently developed as a strategy to stimulate luminescence from lanthanides and actinides elements.[18-26] The mechanism of the energy or charge transfer between M chromophores and actinide elements is related with the bonding nature between them.[19, 22, 27] The unsupported An-M complexes are good candidates for these optical applications and for that reason is necessary a good description of the bonding and electronic structure of molecules that involve actinides and transition metals.

In the present work the authors perform a series of calculations to characterize theoretically the bonding nature of a series of complexes with general structure $[Cp_2ThMCp(CO)_2]^+$ where M=Fe, Ru, Os.[3, 4] The synthesis of some of these systems were reported in the late 1980s and there is not a detailed description about its electronic structure and bonding nature, these molecules look like a good model candidates to understand better the optical spectra in An-M unsupported compounds. The work has been divided in three more sections: Models and computational details, Results and discussion and Conclusions.

2. Theoretical Models and Computational Details

All structures and energies were calculated using Amsterdam Density Functional (ADF) code where the relativistic scalar and spin-orbit effects are incorporated by the zeroth-order regular approximation (ZORA Hamiltonian).[28] The complexes were divided logically in two fragments $[Cp_2Th]^{2+}$ and $[MCp(CO)_2]^-$ were M represents the transition metals Fe, Ru and Os. The symmetry of the molecules was assumed C_s (Figure1). With the objective to analyze if the transition metal is in low or high spin ground state the molecular fragment with this element was optimized individually using two different spin polarizations $\Delta\rho$=0 and 2 to modeling in a relativistic scheme the equivalent to a singlet and triplet states. Also the complexes were optimized into the same two spin polarizations, which is important to predict the optical

properties of these molecules and below this is explained in more detail. The BP86 generalized gradient approximation exchange–correlation functional was used with standard Slater type orbital (STO) basis set with triple-ξ quality double plus polarization function for all atoms (TZ2P), this combination of GGA-functionals and basis set had shown to be suitable in the description of the actinide complexes in our previous work.[27] In all cases the frequency calculations were carried out to verify the quality of the minimum found in our optimization process and also the frequencies of carbonyls ligands were used to estimate the nature of the interaction between this ligand and transition metal.[29-31] An analysis of bonding energetics were performed by combining a fragment approach to the molecular structure of a chemical system with the decomposition of the total bonding energy (E_B), according to the Morokuma-Ziegler decomposition, as:

$$E_{BE}=E_{Pauli}+E_{elec}+E_{orb} \quad (1)$$

where E_{Pauli}, E_{elec}, and E_{orb} are, the Pauli repulsion, electrostatic interaction, and orbital-mixing terms, respectively.[32] The electrostatic component is calculated from the superposition of the unperturbed fragment densities at the molecular geometry and corresponds to the classical electrostatic effects associated with coulombic attraction and repulsion have given a detailed description of the physical significance of these properties. The electrostatic contribution is most commonly dominated by the nucleus-electron attractions and therefore has a stabilizing influence. The Pauli component is obtained by requiring that the electronic antisymmetry conditions be satisfied and has a destabilizing character, whereas the orbital-mixing component represents a stabilizing factor originating from the relaxation of the molecular system due to the mixing of occupied and unoccupied orbitals and can involve electron pair bonding, charge-transfer or donor-acceptor interactions, and polarization.[32] Molecular fragments were selected in the same way that was explained before.

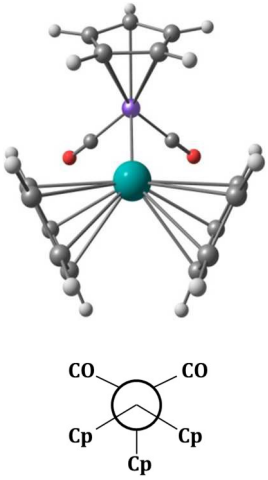

Figure1. Molecular model for the complex. Green and purple represent respectively Th and transition metal TM=Fe, Ru, Os.

Scalar Relativistic Time Dependent Density Functional Theory (SR-TDDFT) was employed to calculate energies for the 30 singlet + 30 triplet excitations, which are used as the basis for the self-consistent two-component spin-orbit coupling TDDFT (SOC-TDDFT) within the ZORA Hamiltonian.[33-35] In all cases at least five spin-mixed excitations were calculated in the full SOC-TDDFT calculations, where the SR-TDDFT results was used as an input, with which the singlet and triplet contributions to the spin-mixed excitation were confirmed. Lowest triplet state were optimized by specifying two unpaired electrons (unrestricted DFT) in a regular geometry optimization with the SR ZORA Hamiltonian with lowered symmetry to reproduce the possible symmetry breaking in the excited triplet state. The GGA SAOP (statistical average of orbitals exchange correlation potential) functional that was specially designed for the calculations of optical properties were used.[36-37] Environmental effects were included via COSMO continuum solvation using dichloromethane parameters.[38-39]

Particularly the main interest with respect to the optical properties of these kinds of compounds are to predict the possible emission induced by charge or energy transfer from the transition metal fragment toward the actinide fragment. Following excitation of the emitter, there are two limiting cases which may be considered and which are a function of the

environment. If the excited state (singlet or triplet) is long lived and the environment reorganization energy is small, the excited emitter will relax on the excited state potential energy surface. However, if the emission process is faster than reorganization, the excited emitter would remain near the ground state singlet geometry. If the former case is true emission can be describe by vertical transition from the ground state singlet at the excited state geometry into the excited state manifold. Of course the presence of the metals centers performs two important roles. First, the SOC increases the intersystem crossing from the excited singlet manifolds (S_n, n>0) to the triplet manifold. This process has been referred to as triplet harvesting and is well documented in the literature. Second the formally spin forbidden T_1-S_0 transition is activated via SOC. In order to accurately predict the absorption and emission energy the geometry employed is critical. Different authors have reported both the optimized excited-state triplet and ground-state singlet geometries with good predictions about optical properties in different transition metal complexes.[27, 40-42]

The radiative rate k_i and radiative lifetime τ_i from substate i (i=1, 2, 3) of the ground excited triplet to the ground state were calculated from the excitation energy ΔE_i and the transition dipole moment M^i with SOC included:

$$k_i = \frac{1}{\tau_i} = \frac{4}{3t_0}\alpha_o{}^3(\Delta E_i)^3 \sum_{\alpha=(x,y,z)}\left|M_\alpha{}^i\right|^2 \quad (2)$$

with $t_0 = (4\pi\varepsilon_0)^2\,\hbar^3/m_e\,e^4$ and α_0 the fine structure constant. In a medium, these are corrected for the refractive index n. According to this correction, our calculated parameters were multiplied by the square of the refractive index of dichloromethane (n =1.42).

The observed radiative lifetime is then an average over the three substates under the assumption fast thermalization:

$$\tau_{av} = \frac{1}{k_{av}} = \left(\frac{3}{k_1+k_2+k_3}\right) \quad (3)$$

or, more accurately, a Boltzmann average when the energy difference between the excited triplet substates is non negligible with respect to the temperature T:

$$\tau_{av} = \frac{1}{k_{av}} = \left(\frac{1+e^{-\left(\frac{\Delta E_{1,2}}{k_B T}\right)}+e^{-\left(\frac{\Delta E_{1,3}}{k_B T}\right)}}{k_1+k_2 e^{-\left(\frac{\Delta E_{1,2}}{k_B T}\right)}+k_3 e^{-\left(\frac{\Delta E_{1,3}}{k_B T}\right)}} \right) \quad (4)$$

with k_B the Boltzmann constant. The last equation at T=300 K was used in the present work[40].

3. Results and Discussion

The chemical structures of the molecules studied are shown in Figure 1. Optimized gas phase geometries were obtained for both the ground-state singlet and first excited triplet states at BP86/TZ2P level of theory. The geometries obtained with the all electron basis set are consistent with previous experimental and theoretical reports in similar systems. Optimized M-Cp (centroid), M-CO and C-O distances for the transition metal fragment and also the most important distances for the complexes are presented in Table 1.

Overall TM fragment is distorted by passing from the singlet ground state to the excited triplet. We observe an increment in all distances upon going from optimized singlet geometry to the triplet in the transition metal fragment; that predict an important Stokes shift if the emission is presented. For the three different metals the ground state was singlet and the increment in the C-O distance evidence the backdonation from metal to the π^* orbitals in CO ligand and the well-known reduction of the frequencies with respect to the free ligand.

Table1. Optimized geometries for $[CpM(CO)_2]^-$ fragment and $[Cp_2AnMCp(CO)_2]^+$ complexes. All distances are in angstrom (Å) and frequencies in cm^{-1}

	Fe		Ru		Os	
$[CpM(CO)_2]^-$	**Δρ=0***	**Δρ=2**	**Δρ=0**	**Δρ=2**	**Δρ=0**	**Δρ=2**
d(M-Cp)	1.570	2.093	1.993	2.225	1.996	2.166
d(M-CO)	1.715	1.803	1.844	1.868	1.844	1.850
d(CO)	1.178	1.175	1.175	1.179	1.180	1.191
ν(sym)	1860.	1872.	1881.	1810.	1875.	1776.
ν(asym)	1752.	1719.	1770.	1716.	1761.	1685.
$[Cp_2ThMCp(CO)_2]^+$						
d(Th-M)	2.738	2.907	2.837	3.041	2.893	3.073

d(Th-Cp)	2.516	2.478	2.517	2.484	2.514	2.484
d(M-Cp)	1.745	1.740	1.988	1.932	1.984	1.937
d(M-CO)	1.742	1.762	1.875	1.895	1.874	1.892
d(CO)	1.169	1.159	1.1673	1.158	1.171	1.161
ν(sym)	1929.	1976.	1940.	1980.	1936.	1973.
ν(asym)	1865.	1922.	1868.	1922.	1862.	1913.

* Δρ represents the spin polarization.

These geometrical variations are related with the reordering of the charge due to the interaction between both fragments. To have a complete scheme about these structural modifications and to get a more realistic idea with respect to the charge reordering mentioned above, it is necessary to understand the nature of the interaction between the molecular fragments. An analysis of the molecular orbitals in these complexes shows that the bonding interaction involve a σ-donation from the HOMO orbitals in $[CpM(CO)_2]^-$ fragment toward $[Cp_2Th]^{2+}$. Figure 2 shows the molecular orbital diagram for $[Cp_2ThRuCp(CO)_2]^+$ complex; here it is possible to see the σ-orbital interactions that stabilize the system. That is not the only one orbital interaction, we also found a π-donation from the lone pairs in the transition metal into the π accepting orbital in the actinide ion, but this is inner in energy. In this work we are interested in the optical properties and the possible Stokes shift due to geometry distortion, then for our interest is better analyze the most external σ-donation. The bonding orbitals in the molecule are mainly a result of electron donation from HOMO in the $[CpRu(CO)_2]^-$ fragment, which have 68% d and 13% s character of Ru atom, to empty orbitals in Cp_2Th fragment which involve *f* orbitals of the Th atom. This σ-bonding orbital represents the HOMO in the complex, that allow us to explain the important geometrical changes in the excited states explained above taking into account the reduction in the bonding character of this orbital when an electron is removed from the molecular HOMO to an excited position.

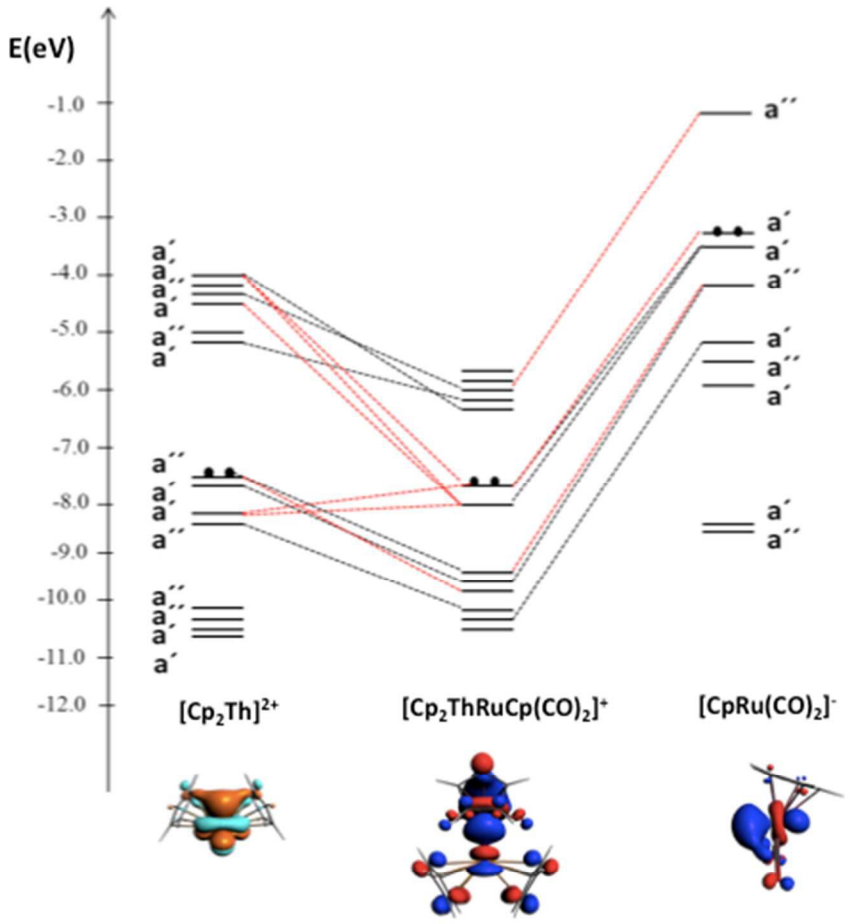

Figure 2. Molecular orbital diagram (energies in eV) for $[Cp_2ThRuCp(CO)_2]^+$ complexes. The molecular orbitals in the fragments that originate the HOMO σ-bonding orbital in the molecule are shown.

Also it is observed the back-donation mainly from the HOMO in $[Cp_2Th]^{2+}$ toward the Ru fragment. This back-donation occur mainly by charge transfer between locally π and δ molecular orbitals in the $[Cp_2Th]^{2+}$ fragment with orbitals in the other fragment, in both cases these molecular orbitals have a low contribution of metals and are predominantly orbitals located in the ligands. Then the metal structure is not significantly affected by this interaction.

The scheme explained suggests that the interaction between both fragments have some covalent character but is not conclusive about the nature of the interaction. To get a global

representation of the bond we use the energy decomposition of the An-M bonding based on the Morokuma-Ziegler scheme. In Table 2 the result of this energy decomposition are presented. For the three complexes the orbital contribution to the bonding energy represent 25, 24 and 23% respectively, of the total electrostatic and orbital contributions to the total attractive interaction and clearly indicate that the electrostatic contributions dominate the Th-M interaction. However the orbital contribution is not insignificant. Clearly charge transfer occurs on Th-M bond formation, however the orbital term most likely represent a strong charge rearrangement that occurs in the $[CpM(CO)_2]^-$ fragment, resulting from internal polarization as a consequence of its interaction with the charge distribution in the Th fragment.

Table 2. Bonding energy decomposition analysis (all values in eV).

Molecule*	E_{Pauli}	E_{elec}	E_{orb}	BE	$\%E_{elec}$	$\%E_{orb}$
$[Cp_2ThFeCp(CO)_2]^+$	7.63	-14.66	-4.85	-11.88	75	25
$[Cp_2ThRuCp(CO)_2]^+$	8.39	-15.43	-4.78	-11.82	76	24
$[Cp_2ThOsCp(CO)_2]^+$	8.27	-15.57	-4.66	-11.96	77	23

*The BE represent the interaction energy between the $[Cp_2Th]^{2+}$ and $[CpM(CO)]^-$ molecular fragments.

Spectroscopic Properties

The electronic properties discussed above have a direct influence over the spectroscopic properties of the molecules investigated here. The first calculated property was the vibrational frequencies, first to corroborate the quality of the minimum obtained and second to evidence the electron transfer analyzing the vibrational frequency of the carbonyl ligands. In Table 1 these results are presented.

In all cases the frequencies were positive indicating that the geometries obtained are in a true minimum. In the other hand the comparison between theoretical values of the CO frequency with experimental available results show good correlation between them. The value of the frequency in the molecules is consistent with the fact that the backdonation to π^* empty molecular orbitals in CO (free ν_{CO} = 2143 cm^{-1}) reduce the bond order in the ligand and as consequence the frequency is lower than in the free ligand. Also, in all cases the CO bond

distance for this ligand is slightly larger than the value for free ligand (1.137 Å calculated at the same level), which is consistent with the model of the bonding, described above.

We also calculated the electronic transitions. In this point it is important to take into account that the normal selections rule, which forbidden the spin flip transitions, need a reformulation when spin-orbit interaction is considered. The molecular spinors have a contribution of both kind of spin functions |α> and |β> and due to that the spin flip transitions are allowed in these cases. In our case we consider both situations SR-TDDFT/ZORA and SO-TDDFT/ZORA levels of calculations to describe the absorption spectra of the molecules considered here. In Table 3 appear the most important electronic transitions for $[Cp_2ThMCp(CO)_2]^+$ complexes; in all cases we calculated the singlet (S) → singlet (S) and singlet (S) → triplet (T) (at SR level). As can be seen when the spin-orbit interaction is considered the spin flip transitions represented by $a_{1/2} \rightarrow a_{1/2}^*$ have a low value of oscillator strengths but are not forbidden. Another important result is that all these transitions implies a promotion of one electron from a molecular orbital centered on the M (Fe, Ru, Os) fragment toward the fragment containing the Th atom, with this, the actinide sensitization by transition metal is guaranteed. In general the position of the electronic transition is similar at both level of calculations with a slightly shift at SO-ZORA level. Based on experimental reports and theoretical predictions for the similar molecules, where exist a direct bond between actinide or lanthanide element with a transition metal in the presence of similar ligands, and where UV-visible studies reveal a luminescent behavior, we propose in the present study the possible emission of these Th complexes.[43-45]

Table 3. Most important electronic transitions for $[Cp_2ThMCp(CO)_2]^+$ complexes.

Molecule			λ(nm)	f	Origin	Assignment
$[Cp_2ThFeCp(CO)_2]^+$	**ZORA**	S→S	574.4	$7.0*10^{-4}$	HOMO→LUMO	Fe→Th
			361.5	$7.5*10^{-3}$	HOMO-4→LUMO	
		S→T	**593.5**	**-**	**HOMO→LUMO**	
	ZORA+SO		**604.5**	**$3.8*10^{-6}$**	**HOMO($a_{1/2}$)→LUMO($a_{1/2}$*)**	Fe→Th
			445.5	$5.2*10^{-3}$	**HOMO($a_{1/2}$)→LUMO+1($a_{1/2}$)**	
$[Cp_2ThRuCp(CO)_2]^+$	**ZORA**	S→S	414.8	$6.1*10^{-3}$	HOMO-1→LUMO	Ru→Th
			349.6	$1.2*10^{-2}$	HOMO-3→LUMO	
		S→T	**533.5**	**-**	**HOMO→LUMO**	Ru→Th
	ZORA+SO		**542.9**	**$3.0*10^{-6}$**	**HOMO($a_{1/2}$)→LUMO($a_{1/2}$*)**	Ru→Th
			421.7	$5.7*10^{-3}$	HOMO-1($a_{1/2}$) →LUMO($a_{1/2}$)	
			352.9	$9.6*10^{-3}$	HOMO-3($a_{1/2}$) →LUMO($a_{1/2}$)	
$[Cp_2ThOsCp(CO)_2]^+$	**ZORA**	S→S	418.1	$5.0*10^{-3}$	HOMO-1→LUMO	Os→Th
			351.9	$1.2*10^{-2}$	HOMO-3→LUMO	
		S→T	**570.4**	**-**	**HOMO→LUMO**	
	ZORA+SO		**581.0**	**$2.7*10^{-4}$**	**HOMO($a_{1/2}$*)→LUMO($a_{1/2}$)**	Os→Th
			434.3	$4.7*10^{-3}$	**HOMO-1($a_{1/2}$)→LUMO($a_{1/2}$)**	

Table 4 summarizes our theoretical results, which contribute to explain the possible emission proposed here. The calculations were done in vacuum and adding the effect of the environment through a COSMO model. One important parameter calculated was the Zero-Field-Splitting (ZFS) for the lowest excited triplet. Normally due to SOC the triplet state is split into three substates, for a symmetry higher than C_3 this three states are separated by symmetry into an A and E states. In the present case due to the symmetry reduction the three states are not degenerate and the ZFS was determined as the energy difference between them. The first important result in the complexes studied here was the relatively large value for the ZFS in the three complexes originated by a strong SOC, which means that at least one triplet substate has some singlet character, with a consequent more probability for emission to the ground state. That is evident in Table 4, the third transition in all cases has more than 5% of contribution to the singlet states and the oscillator strength is two or three orders of magnitude larger than the values for the other two substates. The ZFS value increases when the solvent

effect is included in the calculations; on average the ZFS increases around 30 cm^{-1} for Fe and Ru complexes and 20 cm^{-1} for Os complex. In the same way the radiative lifetime τ_{av} is reduced in one order of magnitude for Fe and Ru (first value in Table 4) cases when the solvent is included, for Os complex the order of magnitude do not change. In all cases the lifetimes obtained using both approximations in Equations 3 and 4 are completely different in magnitude. Unfortunately the experimental results for these kinds of complexes are very few and our results have a predictable value only. However all the results obtained here are in agreement with previous theoretical reports.

Table 4. Calculated emission properties of $[Cp_2ThMCp(CO)_2]^+$ complexes

Molecule	λ(nm)	f	ZFS(cm^{-1})	τ_{av}(s) [a]	Assignation[b]
$[Cp_2ThFeCp(CO)_2]^+$	1132.8	$9.4*10^{-8}$			Th→Fe (LUMS→HOMS) 100% T
SO-TDDFT/Vacuum	1132.4	$7.5*10^{-7}$	45.2	$2.13*10^{-3}$	100% T
	1126.8	$2.6*10^{-5}$		$2.05*10^{-1}$	97% T + 3% S
	837.1	$1.4*10^{-7}$			Th→Fe (LUMS→HOMS) 100% T
SO-TDDFT/COSMO	836.6	$1.6*10^{-5}$	73.4	$2.93*10^{-4}$	100% T
	831.8	$9.0*10^{-5}$		$7.42*10^{-2}$	94% T + 6% S
$[Cp_2ThRuCp(CO)_2]^+$	1178.5	$1.7*10^{-7}$			Th→Ru (LUMS→HOMS) 100% T
SO-TDDFT/Vacuum	1178.0	$2.3*10^{-8}$	54.8	$2.10*10^{-3}$	100% T
	1170.7	$2.0*10^{-5}$		$1.22*10^{-1}$	97% T + 3% S
	830.3	$2.1*10^{-6}$			Th→Ru (LUMS→HOMS) 100% T
SO-TDDFT/COSMO	829.7	$1.6*10^{-5}$	88.4	$2.26*10^{-4}$	100% T
	823.9	$1.2*10^{-4}$		$5.00*10^{-1}$	92% T + 8% S
$[Cp_2ThOsCp(CO)_2]^+$	1095.1	$2.4*10^{-8}$			Th→Os (LUMS→HOMS) 100% T
SO-TDDFT/Vacuum	1094.5	$1.3*10^{-8}$	58.9	$7.59*10^{-4}$	100% T
	1092.5	$7.0*10^{-5}$		$7.56*10^{-1}$	97% T + 3% S
	796.1	$3.1*10^{-7}$			Th→Os (LUMS→HOMS) 100% T
SO-TDDFT/COSMO	795.5	$1.6*10^{-5}$	80.9	$3.97*10^{-4}$	100% T

	790.7	$5.5*10^{-5}$	$3.12*10^{-2}$	94% T + 6% S

[a] The first value for the lifetime was obtained from Eq 3 and the second using Eq 4

[b] All the transitions occurs from the Low Occupied Molecular Spinor (LUMS) to the High Occupied Molecular Spinor (HOMS). In all cases the contribution of the Triplet and Singlet to the transition appears in percent.

As it was explained above the distances between metals and ligands do not change considerably in the excited state; the geometrical parameter with the most important changes is the Th-M distance, thus we can assume that the stretching vibration between both metals is responsible for the vibronic coupling with the excited states. In general the emission wave lengths predicted in the calculation appear over 700 nm and the increment of the position occur in the order Os < Ru < Fe. In Table 4 these values are presented for all the molecules. The changes in the excited state geometry introduce an important Stokes shift in all cases.

4. Conclusions

Zero Field Splitting (ZFS) and radiative lifetime (τ_{av}) are important photophysical properties for the excited states, particularly for the first excited triplet. These parameters are crucial to design more efficient compounds for technological applications and in the present work we pointed out the use of theoretical tools to predict the possible emission in heterobimmetallic compounds with direct metal-metal interaction where one metal center is a transition metal and the other an actinide element. Even when the experimental reports are few for these kind of molecules, the present work represent an step in the description of the optical properties in model compounds with structural and physical properties desirable in molecular engineering using a high level of theory. The molecules under study in the present work have an important unsupported metal-metal interaction, which is determined by some degree of covalence of the chemical bond in all cases (around 25%), but for the three cases studied, the most important interaction between Th and transition metal is ionic. Also the SOC-ZORA calculation shows the possible emission of the Th complexes. The relatively large value of ZFS introduces some singlet contribution into the substates of the first excited triplet, increasing the emission probability. The antenna effect model can be used to justify the sensitization of the actinide element by a transition metal complex. These calculations show that the $[CpTM(CO)_2]^-$ fragments bound to the actinide complex are important to obtain a possible NIR emission, being the order of the red shift Os < Ru < Fe with an important Stokes shift .

5. Acknowledgments

We acknowledge fundings from Grant Nos. FONDECYT 1150629, FONDECYT 11140294, Millennium Nucleus RC120001 Iniciativa Científica Milenio del Ministerio de Economía, Fomento y Turismo del Gobierno de Chile. P.C.L. acknowledges CONICYT PCHA/Doctorado Nacional/2013-63130118 for his PhD fellowship.

6. References

1. Gardner, B. M.; Patel, D.; Cornish, A. D.; McMaster, J.; Lewis, W.; Blake, A. J.; Liddle, S. T. *Chem. Eur. J.* **2011**, 17, 11266 – 11273.
2. Mills, D. P.; Liddle, S. T. *Dalton Trans.* **2009**, 5592–5605.
3. Sternal, R. S.; Brock, C. P.; Marks, T. J. *J. Am. Chem. Soc*. **1985**, 107, 8270-8272.
4. Sternal, R. S.; Marks, T. J. *Organometallics*. **1987**, 6, 2621-2523.
5. Chatelain, L.; Walsh, J. P.; Pécaut, J.; Tuna, F.; Mazzanti, M. *Angewandte Chemie*.**2014**, 53, 13434-13438..
6. Mougel, V. ; Chatelain, L. ; Hermle , J. ; Caciuffo , R.; Colineau , E. ; Tuna , F. ; Magnani, N. ; Geyer, A. ; Pécaut , J ; Mazzanti , M. *Angewandte Chemie*.**2014**,53,819-823.
7. Gardner, B. M.; Patel, D.; Cornish, A. D.; McMaster , J.; Lewis, W.; Blake, A. J.; Liddle, S. T. *Chem. Commun.* **2011**,47, 295–297.
8. Liddle, S. T. *R. Soc. A* .**2009**,465, 1673–1700.
9. Liddle, S. T.; McMaster, J. ; Mills, D. P. ; Blake , A. J. ; Cameron , J. ; Woodul ,W. D. *Angewandte Chemie*. **2009**, 48, 1077–1080.
10. Ward, A. L.; Lukens,W. W.; Lu, C. C.; Arnold, J. *J. Am. Chem. Soc*. **2014**, 136, 3647−3654.
11. Roesky, P. W. *Dalton Trans*. **2009**, 1887–1893.
12. Brennan, J. G.; Andersen, R. A.; Robbins, J. L. *J. Am. Chem. Soc*. **1986**, 108, 335–336.
13. Selg, P.; Brintzinger, H. H.; Andersen, R. A.; Horváth, I. T. *Angew. Chem., Int. Ed. Engl*. **1995**, 34, 791–793.
14. Schultz, M.; Burns, C. J.; Schwartz, D. J.; Andersen, R. A. *Organometallics*. **2001**, 20, 5690–5699.
15. Heffern, M. C.; Matosziuk, L.M.; Meade, T. J.*Chem. Rev*. **2014**, 114, 4496−4539.

16. Sykes, D.; Cankut, A. J.; Ali, N. M.; Stephenson, A.; Spall, S. J.; Parker, S. C.; Weinstein, J.; Ward, M.. *Dalton Trans*.**2014**. 43, 6414-6428.
17. Eliseeva, S. V.; Bünzli, J. C. *Chem. Soc. Rev*. **2010**, 39, 189–227.
18. Shaveleev, N .M.; Accorsi, G.; Virgili, D.; Bell, Z. R.; Lazarides, T.; Calogero, G.; Armaroli, N.; Ward, M. D. *Inorg. Chem*. **2005**, 44, 61-72.
19. Chen, F. F.; Chen, Z. Q.; Bian, Z. Q.; Huang, Ch. H. *Coordination Chemistry Review* **2010**, 254, 991-1010.
20. Balzani, V.; Ballardini, R. *Photochemistry and Photobiology* **1990**, 52, 409-415.
21. Ward, M. D. *Coordination Chemistry Review* **2007**, 251, 1663-1677.
22. Hasegawa, Y.; Wada, Y.; Yanagida, S. *Journal of Photochemistry and Photobiology C: Photochemistry Reviews*. **2005**, 5, 183-202.
23. Armelao, L.; Quici, S., Barigelletti, F.; Accorsi, G.; Bottaro, G.; Cavazzini, M.; Tondello, E. *Coordination Chemistry Reviews*. **2010, 254**, 487-505.
24. Monreal, M. J.; Carver, C. T.; Diasconescu, P. L. *Inorg. Chem*. **2007**, 46, 7226.
25. Schelter, E. J.; Veauthier, J. M.; Thompson, J. D.; Scott, B. L.; John, K. D.; Morris, D. E.; Kiplinger, J. L. *J. Am. Chem. Soc*. **2006**, 128, 2198–2199.
26. Pope, S. J. A.; Burton-Pye, B. P.; Berridge, R.; Khan, T.; Skabara, P. J.; Faulkner, S. *Dalton. Trans*. **2006**, 2907-2912.
27. Ferraro, F.; Páez-Hernández, D.; Murillo-López, J. A.; Muñoz-Castro, A.; Arratia-Pérez, R. *J. Phys. Chem. A*. **2013**, 117, 7847-7854.
28. Amsterdam Density Functional (ADF) Code. Release 2008; Vrije Universiteit: The Netherlands 2012.
29. Verluis, L.; Ziegler, T. *J. Chem. Phys*. **1988,** 88, 322-328.
30. Vosko, S. H.; Milk, L.; Nusair, M. *Can. J. Phys*. **1980,** 58, 1200-1210.
31. Perdew, J. P.; Burke, K.; Ernzerhof, M. *Phys. Rev. Lett*. **1996,** 77, 3865-3868.
32. Bickelhaupt, F. M.; Baerends, E. *J. Rev. Comput. Chem*. **2000**, 15, 1-85.
33. Wang. F.; Ziegler. T.; van Lenthe. E.; van Gisbergen. S. J. A.; Barendes. E. J. *J. Chem. Phys*. **2005**, 122, 204103.
34. Wang. F.; T. Ziegler. *J. Chem. Phys*. **2005**, 123, 154102.
35. Younker. J. M.; Dobbs. K. D. *J. Phys. Chem*. **2013**, 117, 25714.
36. Kootstra, F.; Boeij, P. L. ; Snijders, J. G. *J. Chem. Phys*. **2000**, 112, 6517-6532.

37. Romaniello, P.; Boeij, P. L. *Phys. Rev. B.* **2005**, 71, 155108,1-17.
38. Pye. C. C.; Ziegler.T. *Theoretical Chemistry Accounts*. **1999**, 101, 396.
39. Klamt. A. *Journal of Physical Chemistry*. **1995**, 99, 2224.
40. Gritsenko, O. V.; Schipper, P. R.; Baerends, E. *J. Chem. Phys. Lett.* **1999**, 302, 199-207.
41. Smith, A. R. G.; Riley, P. L.; Burn, P. L.; Gentle, I. R.; Lo, S.-C:; Powell, B. J. *Inorg. Chem*. **2012**, 51, 2821-2831.
42. Mori, K.; Goumans, T. P. M.; van Lenthe, E.; Wang, F. *Phys. Chem. Chem. Phys*. **2014**, 16, 14523-14530.
43. Butovskii, M. V.; Döring, V. B.; Wagner, F. R.; Grin, Y.; Kempe, R. *Nature Chemistry*. **2010**, 2, 741-744.
44. Butovskii, M. V.; Tok, O. L.; Wagner, F. R.; Kempe, R. *Angew. Chem. Int. Ed*. **2008**, 47, 6469-6472.
45. Pershagen, E.; Nordholm, J.; Borbas, K. E. *J. Am. Chem. Soc*. **2012**, 134, 9832-9835.